

Equation of State for Strongly Coupled Systems with Emerging Bound States

Shuai Y.F. Liu and Ralf Rapp¹

¹*Department of Physics and Astronomy and Cyclotron Institute,
Texas A&M University, College Station, TX 77843-3366, USA*

(Dated: December 30, 2016)

Non-perturbative methods play an important role in quantum many-body systems, especially in situations with an interplay of continuum and bound states and/or a large coupling strength between the constituents. One such method in calculating the equation of state of such systems is based on the Luttinger-Ward functional, representing a series of skeleton diagrams with fully dressed propagators. Here we extend the evaluation of this functional by resumming the ladder diagram series using a “matrix log” technique which accounts for dynamically formed bound and resonant states. We illustrate this approach by applying it to the equation of state of the quark-gluon plasma (QGP) employing an interaction kernel constrained by lattice QCD. By fitting lattice-QCD data for the pressure with an effective parton mass parameter, we extract self-consistent parton spectral functions and two-body scattering amplitudes. We find that, as the pseudo-critical temperature (T_{pc}) is approached from above, the quasi-particle peaks in the parton spectral functions dissolve as a consequence of large scattering rates, which in turn are driven by dynamically formed pre-hadronic states. Our results suggest that a gradual emergence of hadronic states is intricately related to the strongly coupled nature of the QGP near T_{pc} .

PACS numbers: 12.38.Mh, 52.27.Gr, 51.30.+i

Keywords: Luttinger-Ward Functional, Grand Potential, T -matrix, Quark-Gluon Plasma

The interplay of bound and continuum states is a key feature in a wide variety of quantum many-body systems, *e.g.*, cold atomic gases [1], electromagnetic and electron-hole plasmas [2, 3], nuclear matter [4, 5], and its transition to the quark-gluon plasma (QGP) [6–8]. A microscopic description of their equation of state (EoS) becomes particularly challenging when a strong coupling between the constituents mandates methods beyond the quasi-particle approximation. One such method is the Luttinger-Ward-Baym (LWB) formalism [9–11], which allows to evaluate the grand potential in terms of Feynman diagrams with in-medium propagators. The predictive power of this formalism hinges on including the relevant diagrams in the calculation of the Luttinger-Ward functional (LWF), $\Phi(G)$, where G denotes the dressed single-particle propagator. Typically, $\Phi(G)$ is constructed to finite order in the “skeleton diagram” expansion, from which the integral equation for G should be solved self-consistently [12, 13]. Alternatively, the diagrammatic Monte-Carlo method discussed in Ref. [14] (and references therein) has been shown to yield controlled results for a convergent series of skeleton diagrams. However, for a divergent series, *e.g.*, at large coupling strength, an explicit non-perturbative resummation should be developed. At the single-particle level, the Dyson equation enables to resum large self-energies into the denominator of the propagator function. In two-body channels, the Bethe-Salpeter equation (BSE) iterates t -channel ladder diagrams to all orders encompassing both bound-state formation and scattering states. The self-consistent scheme of self-energy and BSE within the Dyson-Schwinger framework, or within more tractable approximations such as the thermodynamic T -matrix ap-

proach [2], can be implemented into the LWB formalism. However, a pertinent resummation of the LWF is less straightforward. It can be carried out for special cases, *e.g.*, separable interaction kernels [5], but we are not aware of a general procedure for non-separable interactions. In the present paper, we put forward a generalized T -matrix approach which resums the LWF for an arbitrary kernel while fully accounting for quantum effects, in particular large collisional widths in the one- and two-body spectral functions. To illustrate this method, we apply it to the QGP, thereby providing insights into its (non-) quasi-particle structure and the role of hadron-like correlations near the pseudo-critical temperature, T_{pc} .

We start from the expression of the grand potential as a functional of the full propagator G ,

$$\Omega(G) = \mp \text{Tr} \{ \ln(-G^{-1}) + (G_0^{-1} - G^{-1})G \} \pm \Phi(G), \quad (1)$$

where the trace (Tr) indicates summations and integration over Matsubara frequencies (ω_n), 3-momentum (\mathbf{p}) and internal degrees of freedom such as spin; G_0 denotes the bare propagator. The single-particle self-energy can be expressed as a functional derivative of the LWF,

$$\Sigma(G) = \beta \delta \Phi(G) / \delta G, \quad (2)$$

where $\Phi(G)$ is usually constructed by a skeleton expansion to finite loop order [12]. Here we consider a situation where the self-energy $\Sigma(G)$ is calculated from a T -matrix (or BS) amplitude with kernel V , with formal solutions

$$T = V + VGGT = (1 - VGG)^{-1}V \quad (3)$$

$$\Sigma(G) = TG = (1 - VGG)^{-1}VG. \quad (4)$$

As mentioned above, a non-perturbative resummation of $\Phi(G)$ corresponding to the self-energy $\Sigma(G)$ is not known for a general potential. However, it turns out that Eq. (2) can be formally integrated, together with Eq. (4), as

$$\begin{aligned}\Phi(G) &= \frac{1}{\beta} \int dG (1 - VGG)^{-1} VG = -\frac{1}{2\beta} \ln(1 - VGG) \\ &= \frac{1}{2\beta} \left\{ VG + \frac{1}{2} VGGVG + \dots + \frac{1}{\nu} VGG \dots VG \right\} G .\end{aligned}\quad (5)$$

The second line recovers the standard skeleton expansion,

$$\Phi(G) = \frac{1}{2} \text{Tr} \sum_{\nu=1}^{\infty} \frac{1}{\nu} \Sigma_{\nu}(G) G , \quad (6)$$

where $\Sigma_{\nu}(G)$ represents the ν^{th} order in the skeleton diagram, expressed as a functional of G [9]. The combinatorial factor $1/\nu$ prevents a straightforward resummation of the skeleton expansion. The formally integrated form in the first line of Eq. (5) is a non-perturbative expression which remains finite for large V , for which the perturbative series in the second line is usually divergent. This calls for a practical method of carrying out the functional integral in Eq. (5).

Toward this end we resolve the above functional expression into discrete energy-momentum indices (similar to the discretization of the T -matrix integral equation introduced in Ref. [15]), and convert the log-function into a matrix representation. Considering 4-momentum as a single discretized variable, one can write the 2-body interaction kernel and single-particle propagators as

$$\begin{aligned}\mathbb{V}_{ij} &\equiv V(\tilde{k}_i, \tilde{k}_j) \\ \mathbb{G}_{ij} &\equiv G(\tilde{k}_i) \delta_{ij} , \quad \mathbb{G}(\tilde{P})_{ij} \equiv G(\tilde{P} - \tilde{k}_i) \delta_{ij} ,\end{aligned}\quad (7)$$

where $\tilde{k}_{i,j} = (i\omega_n, \mathbf{k})_{i,j}$ are relative in- and outgoing 4-momenta in Matsubara representation, and \tilde{P} is the total 2-particle 4-momentum in the heat bath. This recovers the standard inverse-matrix solution [15] to the T -matrix,

$$\mathbb{T}(\tilde{P}) = [\mathbb{1} - \mathbb{V}\mathbb{G}\mathbb{G}(\tilde{P})]^{-1} \mathbb{V} , \quad (8)$$

with $T(\tilde{p}, \tilde{q}|\tilde{p}', \tilde{q}')$ written as $T(\tilde{P} - \tilde{k}_i, \tilde{k}_i|\tilde{P} - \tilde{k}_j, \tilde{k}_j) = \mathbb{T}(\tilde{P})_{ij}$. The key point is now to evaluate the logarithm in Eq. (5) by a matrix logarithm, denoted by “Log”, as

$$\Phi = -\frac{1}{2} \int d^4 \tilde{P} \text{Tr} \left\{ \text{Log} \left[\mathbb{1} - \mathbb{V}\mathbb{G}\mathbb{G}(\tilde{P}) \right] \right\} . \quad (9)$$

The “Tr” of the matrix includes relative 4-momentum and internal degrees of freedom, and is followed by a scalar integration over \tilde{P} . Equation (9) constitutes a practical formula to compute the LWF exactly; it is an example of a primitive functional of $\Sigma(G)$, *i.e.*, a category of functional integrals which can be carried out by

a matrix function.

A convenient way to implement the Log operation is to recast the LWF as

$$\Phi = \frac{1}{2} \int d^4 \tilde{p} \ln \Sigma(\tilde{p}) G(\tilde{p}) . \quad (10)$$

This can be seen by augmenting the Log in Eq. (9) with $1 = [\mathbb{G}\mathbb{G}(\tilde{P})]^{-1} [\mathbb{G}\mathbb{G}(\tilde{P})]$ and combining it with the first (inverse) factor to obtain

$$\text{LogT}(\tilde{P}) = -\text{Log} \left[\mathbb{1} - \mathbb{V}\mathbb{G}\mathbb{G}(\tilde{P}) \right] [\mathbb{G}\mathbb{G}(\tilde{P})]^{-1} . \quad (11)$$

Writing $\text{LogT}(\tilde{P})_{ij} = \ln T(\tilde{P} - \tilde{k}_i, \tilde{k}_i|\tilde{P} - \tilde{k}_j, \tilde{k}_j)$, one can contract the diagonal (forward-scattering) T -matrix with one propagator, G , to define

$$\ln \Sigma(\tilde{p}) \equiv \int d^4 \tilde{q} \ln T(\tilde{p}, \tilde{q}|\tilde{p}, \tilde{q}) G(\tilde{q}) , \quad (12)$$

which, together with the remaining propagator G , recovers Eq. (10); note the formal similarity of Eq. (10) with the skeleton expansion, Eq. (6). With this setup, the only change in going from the self-consistent self-energy,

$$\Sigma(\tilde{p}) = \int d^4 \tilde{q} T(\tilde{p}, \tilde{q}|\tilde{p}, \tilde{q}) G(\tilde{q}) , \quad (13)$$

to the LWF is replacing the inverse-matrix solution for T from Eq. (8) by the matrix-logarithm, $\ln T$ from Eq. (11) (and the factor \mathbb{V} by $\mathbb{G}\mathbb{G}^{-1}$). Thus, standard approximations and numerical techniques used to calculate the T -matrix can be directly applied to calculate $\ln T$, such as 3D reductions to the BSE [16], partial-wave expansions and center-of-mass (CM) approximations [17, 18]. Within such approximations, an alternative derivation of the resummed LWF has been given in Ref. [19].

As an example of this formalism, we consider in the following its application to a strongly coupled QGP. As a mixed Bose-Fermi system it is believed to share many similarities with ultracold atom systems where the interaction strength can be tuned by external magnetic fields [20]. In particular, we systematically implement benchmarks from lattice-QCD (lQCD) [21–25]. Our main assumption is that the relevant interactions can be represented by a potential-like driving kernel. This is inspired by the success of the potential approach to hadron spectroscopy in vacuum [26, 27]. Importantly, this allows to include remnants of the confining force above T_{pc} , for which there is ample evidence from lQCD. The rather large quasi-particle masses obtained in fitting the lQCD EoS [8, 28, 29] near T_{pc} further justify this approach. We start from an effective Hamiltonian

$$\begin{aligned}H &= \sum \sqrt{m^2 + \mathbf{p}^2} \psi^\dagger(\mathbf{p}) \psi(\mathbf{p}) + \\ &\psi^\dagger(\mathbf{P} - \mathbf{p}) \psi^\dagger(\mathbf{P} + \mathbf{p}) V \psi(\mathbf{P} + \mathbf{p}') \psi(\mathbf{P} - \mathbf{p}') ,\end{aligned}\quad (14)$$

where the summation is over momentum (using relativistic kinematics), spin, color and flavor ($N_f=3$ plus gluons; for simplicity we assume spin degeneracy). For the 2-body potential we adopt the ansatz

$$V(\mathbf{p}, \mathbf{p}') = \mathcal{F}^C V_C(\mathbf{q}) B(p, p') + \mathcal{F}^S V_S(\mathbf{q})/R(p, p') \quad (15)$$

where $\mathbf{q} = \mathbf{p} - \mathbf{p}'$ is the 3-momentum transfer and B and R are relativistic corrections detailed in Ref. [30]. For the color factors, $\mathcal{F}^{C,S}$, of the different two-body channels we use Casimir scaling for both Coulomb and string potentials, albeit with absolute values for the latter to maintain a strictly positive string tension [25]. To quantitatively constrain the in-medium potential, we follow Ref. [31] to calculate the static heavy-quark (HQ) free energy, $F_{Q\bar{Q}}(r, T)$, within the T -matrix formalism, which includes imaginary parts in both the 2-body potential and the single-quark propagators (here self-consistently calculated from the T -matrix). The input potential is then adjusted to fit the IQCD data for $F_{Q\bar{Q}}(r, T)$ above T_{pc} employing an in-medium Cornell-type ansatz for the potential [32, 33],

$$V_C + V_S = -\frac{4}{3}\alpha_s \frac{e^{-m_d r}}{r} - \frac{\sigma e^{-m_s r - (c_b m_s r)^2}}{m_s} \quad (16)$$

with an extra term $-(c_b m_s r)^2$ in the exponential to better capture the residual effects of string breaking in the QGP. The screening mass of the string term, $m_s = (c_s m_d^2 \sigma / \alpha_s)^{1/4}$, is obtained from a one loop calculation for the Debye mass of V_S (cf. also Ref. [34]). The infinite distance limit of the color-singlet potential, $-\frac{4}{3}\alpha_s m_d + \frac{\sigma}{m_s}$, turns out to be twice the Fock term for an individual static quark. The parameter values of the self-consistent fit to HQ free energies are $c_b=1.15$, $\alpha_s=0.192-0.0883\ln(T)$, $\sigma=0.273 \text{ GeV}^2$, $m_d=-0.0583 \text{ GeV} + 1.06 T$, and $c_s=0.148$. Compared to our previous work [30], the Casimir-scaled string term enables a better description of the color-octet free energy. We recall that the fit solutions to the self-consistent HQ potential are not (yet) unique [31], but allow for both “weak” and “strong” potentials, where the former are close to the free energy, while latter rise significantly above it providing a larger force. In the spirit of a strong-coupling framework, we here proceed with a “strong” solution.

The remaining task is to solve the model for the EoS. We here do not attempt to explicitly include condensate effects that are likely responsible for the residual string tension above T_{pc} and (part of) the effective parton masses. We, however, fix the ratio of the light-quark to gluon mass by the Fock terms corresponding to the infinite-distance limit of the input potential, *i.e.*, $M_q/M_g=C_F/C_A=4/9$, the ratio of Casimir factors for fundamental and adjoint representations in $SU_c(3)$ (very similar results are obtained when allowing the ratio to approach the perturbative mass ratio, $M_g/M_q =$

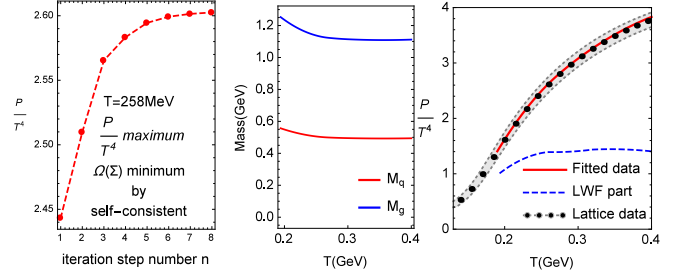


FIG. 1: Evolution of the pressure in the self-consistent iteration procedure (left panel), and temperature dependence of quark and gluon masses (middle panel) needed to fit IQCD data [22] for the scaled pressure, P/T^4 (right panel).

$\sqrt{1/3}/\sqrt{3/4}$ [28] toward high T). This leaves one fit parameter which we adjust to reproduce IQCD data for the pressure. This is done by numerical iteration to self-consistently solve T -matrices and self-energies for a given mass value, $\Sigma(G) = \mathbf{T}G$. We have verified that the iteration procedure, $[G^{(n+1)}]^{-1} = [G_0]^{-1} - \Sigma(G^{(n)})$, where $G^{(n)}$ is the propagator in the n^{th} step, indeed converges to a maximum in the pressure, $P = -\Omega$, cf. Fig. 1 left. This suggests that $G^{n \rightarrow \infty}$ recovers the minimum of the grand potential in our approach, *i.e.*, $\frac{\delta \Omega}{\delta G(\bar{p})} = 0$ is well satisfied at the numerical level.

The temperature dependence of the resulting parton masses (cf. middle panel of Fig. 1) is weaker than in quasi-particle models [35]. In particular, it does not show a large increase toward T_{pc} . Rather, the marked drop in the scaled pressure, P/T^4 (right panel of Fig. 1), is caused by the many-body physics as reflected by the increasing role of the LWF encoding the bound-state contributions [5], suggesting a transition from parton quasi-particles to hadronic degrees of freedom. This interpretation is corroborated upon inspecting the self-consistent spectral functions implicit in the calculation. At low temperature and momentum, the strength in the light-quark spectral functions spreads over an energy region of $\sim 1 \text{ GeV}$, with an on-shell width in excess of the nominal thermal quark mass of $M_q \simeq 0.5 \text{ GeV}$, and a non-Lorentzian shape due to collective low-energy modes, cf. the upper panels of Fig. 2. Thus, low-momentum light quarks are no longer good quasi-particles close to T_{pc} , which, in turn, suppresses their contribution to the pressure. This is different from quasi-particle models [8, 28, 29, 36] where the quark widths are zero or small compared to their masses. Despite the large increase in the degrees of freedom with temperature, the maximum value of the (energy-momentum dependent) width increases by only 25% from $T=194 \text{ MeV}$ to 400 MeV . This is much less than expected from a perturbative behavior, $\Gamma_q \propto g^2 T$, and another manifestation of the increase of the interaction strength as $T \rightarrow T_{pc}$ from above. This increase is in largely driven by the formation of pre-

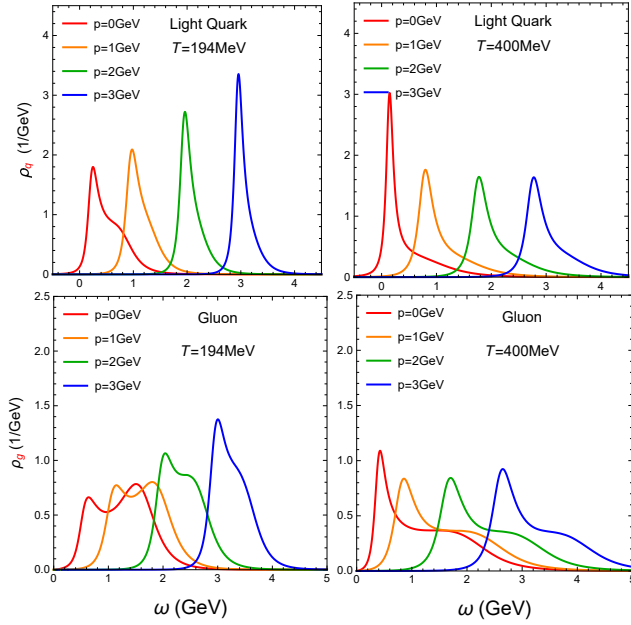


FIG. 2: In-medium spectral functions for quarks (upper panels) and gluons (lower panels) at $T=194$ MeV (left panels) and $T=400$ MeV (right panels) for 3-momenta $p=0-3$ GeV.

hadronic resonance states that emerge in the imaginary part of the quark-anti-quark T -matrix, cf. left panel of Fig. 3. With increasing temperature, the resonances dissolve, which in turn leads to better defined quasi-particles. In this sense, our self-consistent approach exhibits a smooth transition from hadronic to quark degrees of freedom as temperature (or 3-momentum) increases. The color-singlet $q\bar{q}$ bound-state mass of ~ 0.8 GeV near T_{pc} is tantalizingly close to the vacuum ρ -meson mass (the broad spectral function is not unlike results from in-medium hadronic calculations [37]). The situation is similar for gluons (lower panels in Fig. 2) and their interaction amplitudes (right panel in Fig. 3). Their spectral distributions develop low-energy collective modes well below the nominal thermal gluon mass and 2-gluon threshold, respectively.

In summary, we have put forward a non-perturbative resummation technique for the LWF which enables to include the dynamical dissociation and formation of bound states in the EoS of quantum many-body systems self-consistently. This is pertinent to strongly coupled systems where dynamical bound-state effects encoded in the LWF become a leading contribution. We applied this formalism to the QGP at moderate temperatures, by fitting the EoS to lattice-QCD data. The extracted parton spectral functions feature large widths which indicate a melting of the quasi-particle structure at low temperatures and momenta, while being intimately coupled with the emergence of hadronic degrees of freedom. Future tests and applications of this mechanism include

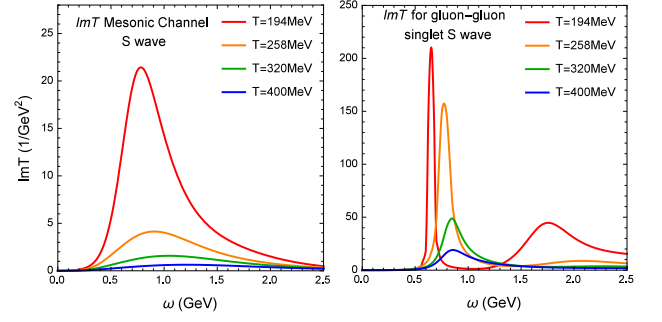


FIG. 3: Imaginary part of the in-medium T -matrix for $P = 0$ in the color-singlet $q\bar{q}$ (left) and gg (right) channels.

quarkonium spectral functions, heavy-quark transport, and quark-number susceptibilities, subject to constraints from lattice-QCD and suitable for implementation into heavy-ion phenomenology. It will also be interesting to deploy this formalism to strongly coupled cold-atom gases, where related mechanisms are believed to be operative [20, 38].

This work is supported by the U.S. NSF through grant no. PHY-1614484.

-
- [1] S. Giorgini, L. P. Pitaevskii, and S. Stringari, *Rev. Mod. Phys.* **80**, 1215 (2008).
 - [2] W.-D. Kraeft, D. Kremp, W. Ebeling, and G. Röpke, *Quantum statistics of charged particle systems* (Springer, 1986).
 - [3] R. Redmer, *Physics Reports* **282**, 35 (1997).
 - [4] M. Schmidt, G. Röpke, and H. Schulz, *Annals of Physics* **202**, 57 (1990).
 - [5] R. Rapp and J. Wambach, *Phys. Lett. B* **315**, 220 (1993).
 - [6] D. Blaschke, F. Reinholz, G. Röpke, and D. Kremp, *Phys. Lett. B* **151**, 439 (1985).
 - [7] J. Hufner, S. P. Klevansky, P. Zhuang, and H. Voss, *Annals Phys.* **234**, 225 (1994).
 - [8] E. V. Shuryak and I. Zahed, *Phys. Rev. D* **70**, 054507 (2004).
 - [9] J. M. Luttinger and J. C. Ward, *Phys. Rev.* **118**, 1417 (1960).
 - [10] G. Baym and L. P. Kadanoff, *Phys. Rev.* **124**, 287 (1961).
 - [11] G. Baym, *Phys. Rev.* **127**, 1391 (1962).
 - [12] J. P. Blaizot, E. Iancu, and A. Rebhan, *Phys. Rev. D* **63**, 065003 (2001).
 - [13] N. Haque, A. Bandyopadhyay, J. O. Andersen, M. G. Mustafa, M. Strickland, and N. Su, *JHEP* **05**, 027 (2014).
 - [14] E. Kozik, M. Ferrero, and A. Georges, *Phys. Rev. Lett.* **114**, 156402 (2015).
 - [15] M. I. Haftel and F. Tabakin, *Nucl. Phys. A* **158**, 1 (1970).
 - [16] R. Woloshyn and A. Jackson, *Nucl. Phys. B* **64**, 269 (1973).
 - [17] M. Mannarelli and R. Rapp, *Phys. Rev. C* **72**, 064905 (2005).
 - [18] F. Riek and R. Rapp, *New J. Phys.* **13**, 045007 (2011).

- [19] S. Y. F. Liu and R. Rapp (2016), 1609.04877.
- [20] T. Sogo, P. Schuck, and M. Urban, Phys. Rev. A **88**, 023613 (2013).
- [21] S. Borsanyi, G. Endrodi, Z. Fodor, A. Jakovac, S. D. Katz, S. Krieg, C. Ratti, and K. K. Szabo, JHEP **11**, 077 (2010).
- [22] A. Bazavov et al. (HotQCD), Phys. Rev. D **90**, 094503 (2014).
- [23] A. Mocsy, P. Petreczky, and M. Strickland, Int. J. Mod. Phys. A **28**, 1340012 (2013).
- [24] O. Kaczmarek, PoS **CPOD07**, 043 (2007).
- [25] P. Petreczky and K. Petrov, Phys. Rev. D **70**, 054503 (2004).
- [26] S. Godfrey and N. Isgur, Phys. Rev. D **32**, 189 (1985).
- [27] S. Capstick and N. Isgur, Phys. Rev. D **34**, 2809 (1986).
- [28] P. Levai and U. W. Heinz, Phys. Rev. C **57**, 1879 (1998).
- [29] S. Plumari, W. M. Alberico, V. Greco, and C. Ratti, Phys. Rev. D **84**, 094004 (2011).
- [30] F. Riek and R. Rapp, Phys. Rev. C **82**, 035201 (2010).
- [31] S. Y. F. Liu and R. Rapp, Nucl. Phys. A **941**, 179 (2015).
- [32] E. Megias, E. Ruiz Arriola, and L. Salcedo, JHEP **0601**, 073 (2006).
- [33] E. Megias, E. Ruiz Arriola, and L. Salcedo, Phys. Rev. D **75**, 105019 (2007).
- [34] Y. Burnier, O. Kaczmarek, and A. Rothkopf, JHEP **12**, 101 (2015).
- [35] A. Peshier and W. Cassing, Phys. Rev. Lett. **94**, 172301 (2005).
- [36] H. Berrehrah, E. Bratkovskaya, T. Steinert, and W. Cassing, Int. J. Mod. Phys. E **25**, 1642003 (2016).
- [37] R. Rapp, J. Wambach, and H. van Hees, Landolt-Bornstein **23**, 134 (2010).
- [38] Y. Ohashi and A. Griffin, Phys. Rev. Lett. **89**, 130402 (2002).